iScience

CellPress
OPEN ACCESS

Review

Ice-binding proteins and bioinspired synthetic mimics in non-physiological environments

Elizabeth A. Delesky[1] and Wil V. Srubar III[1,2,*]

SUMMARY

Ice-binding proteins (IBPs) are produced by a variety of organisms to prevent internal damage caused by ice crystal growth. Synthetic analogs are being designed to mimic beneficial properties of IBPs while mitigating drawbacks related to the use of biological proteins. While a multitude of engineering applications could benefit from the inhibition and control of ice formation and growth, synthetic analogs tend to be less potent than biological IBPs, and both IBPs and synthetic analogs tend to exhibit lower performance in non-physiological (*i.e.*, non-biological) solutions. This review examines the ice interaction properties and performance of IBPs and their synthetic analogs in non-physiological environments. Common methods to measure ice interactions are discussed (*i.e.*, thermal hysteresis, ice recrystallization inhibition, ice growth rate, and ice nucleation). A quantitative meta-analysis of material performance in non-physiological environments is presented, along with a discussion of future research directions. The findings presented herein can inform IBP and synthetic mimic selection to control ice interactions in a wide variety of materials science and engineering applications, including cell, tissue, and organ cryopreservation, food storage and transport, freeze-thaw damage of cementitious materials, and anti-icing surfaces for aerospace vehicles, solar panels, and wind turbines.

INTRODUCTION

Water is a common and readily available solvent used in most industrial fields from medicine to infrastructure (United States Geological Survey, 2022). However, water has unique chemical and physical properties, such as expanding by 9% upon crystallization (Eisenberg and Kauzmann, 2005; Voitkovskii, 1960), which can cause a multitude of issues for materials or systems containing it. For example, during cryopreservation, ice expansion can damage proteins (Kasper and Friess, 2011; Arakawa et al., 2001; Jiang and Nail, 1998; Costantino and Pikal, 2004) or rupture cells (Gao and Critser, 2000; Harding, 2004; Morris and Acton, 2013). In food preservation, the formation and growth of crystallites can alter the texture of foods, rendering them unpalatable (Kaleda et al., 2018; Soukoulis and Fisk, 2016; Kiani and Sun, 2011). In infrastructure, the cyclic freeze-thaw of ice within concrete can induce cracking and failure (Scherer and Valenza, 2005; Scherer, 1999; Liu et al., 2014; Rahman and Grasley, 2014; Yang et al., 2015). Preventing ice growth-induced damage can extend the service life of many engineered materials, saving money, resources, and time in the process.

Ice-binding proteins (IBPs)

Nature has evolved an effective strategy to mitigate the potentially detrimental effects of ice formation within organisms. Ice-binding proteins (IBPs) are a robust series of proteins found in a wide array of organisms, ranging from plants (Hincha and Zuther, 2020; Duman and Olsen, 1993; Griffith et al., 1992; Moffatt et al., 2006), fungi (Duman and Olsen, 1993; Hoshino et al., 2003; Xiao et al., 2010), fish (Marshall et al., 2004; DeVries, 1988; Fletcher et al., 1987; Hew et al., 1981; Slaughter et al., 1981; Davies et al., 1988), insects (Graethert et al., 2000; Liou et al., 1999; Graham and Davies, 2005; Li et al., 1998; Duman et al., 2004), and microbes (Duman and Olsen, 1993; Vance et al., 2018; Garnham et al., 2008; Gilbert et al., 2004). These proteins emerged through convergent evolution and, thus, display a variety of structures, amino acid sequences, and ice interaction residues (Davies, 2014; Dolev et al., 2016). Although the structures of IBPs vary, most IBPs exhibit regular helices with spacing that matches the lattice structure of ice.

[1]Materials Science and Engineering Program, University of Colorado Boulder, Boulder, CO 80309, USA

[2]Department of Civil, Environmental and Architectural Engineering, University of Colorado Boulder, ECOT 441 UCB 428, Boulder, CO 80309, USA

*Correspondence: wsrubar@colorado.edu

https://doi.org/10.1016/j.isci.2022.104286

This is an open access article under the CC BY-NC-ND license (http://creativecommons.org/licenses/by-nc-nd/4.0/).

A subclass of IBPs called antifreeze proteins (AFPs) exhibit similar ice interaction properties, namely: (1) thermal hysteresis (TH), defined as a non-colligative depression of freezing point while maintaining (or elevating) the melting point; (2) dynamic ice shaping (DIS) (*i.e.*, a reshaping of the 1H hexagonal ice crystal structure to form less disruptive ice geometries); and (3) ice recrystallization inhibition (IRI) (*i.e.*, a property that limits ice recrystallization through Ostwald ripening and reduces mean ice crystal size) (Voets, 2017).

Some IBPs exhibit a unique property known as ice nucleation, wherein ice formation is actually promoted due to the presence of the protein. This subclass of IBPs is typically called ice-nucleating proteins (INPs), which often exhibit similar ice interaction mechanisms as AFPs. However, INPs are typically much larger in size, which leads to a change in function (Dolev et al., 2016).

For more information on IBP function, structure, and mechanistic theories, comprehensive reviews have been published in the literature (Dolev et al., 2016; Davies, 2014). The exact mechanism by which IBPs inhibit ice growth has not yet been fully explicated due to the sheer variety of IBPs. However, the prevailing mechanism that is widely agreed-upon postulates that ice interaction is facilitated by an array of quasi-liquid anchored clathrate-waters at the ice-IBP interface that aligns with the crystal lattice of ice (Davies, 2014; Garnham et al., 2011; Chakraborty and Jana, 2018; He et al., 2018). Early genetic mutation studies demonstrated that polar residues play a critical role at the ice-IBP interface (Jia et al., 1996; Zhang et al., 2004; Deluca et al., 1998; Baardsnes et al., 1999; Baardsnes and Davies, 2002; Haymet et al., 1998), and molecular dynamics studies have since supported the hypothesis that bound clathrate waters are present when IRI-active molecules interact with ice crystals (Hudait et al., 2018; Zanetti-Polzi et al., 2019; Grabowska et al., 2018). Other studies have substantiated the important role that hydrophobicity has on the efficacy of ice-binding residues and their interaction at the ice-IBP interface (Baardsnes and Davies, 2002; Stubbs et al., 2017, 2019; Balcerzak et al., 2013). Despite these advances, further fundamental understanding related to ice-IBP interactions is required to fully explicate a universal theory (or theories) of ice interaction.

As an emerging biotechnology, IBPs have the potential to extend beyond biological applications to meet antifreeze needs of other industries in aerospace (*e.g.*, cryogenic fluids), civil engineering (*e.g.*, frost-resistant pavements) (Frazier et al., 2020; Qu et al., 2020), and energy infrastructure (*e.g.*, anti-icing coatings). However, widespread use of IBPs for large-scale applications is limited due to (1) loss of functionality in different non-physiological environments, (2) limited yield for up-scaled IBP production, and (3) rapid expansion upon freezing. According to available literature, IBPs are most commonly studied in solutions that mimic their native physiological environments. These environments have a pH between ~6 and ~8 and contain minimal concentrations of salts and sugars. Proteins are well known to restructure (*e.g.*, denature, aggregate, and degrade) in non-physiological media (Ptitsyn, 1987), thus rendering them ineffective in those environments. Changes in pH and ionic concentration can affect the activity of IBPs. Previous research has attempted to increase yield for IBP production (*e.g.*, 200 mg of IBP from a 5 L recombinant batch of yeast growth (Tab et al., 2018), or 4.6 mg of IBP from 100 g of *Tenebrio molitor* larvae) (Tomalty et al., 2019). However, the quantity of protein produced (<1 g) would be insufficient for large-scale applications. Finally, most IBPs demonstrate TH activity with a rapid and destructive ice "burst" when reaching their new non-equilibrium freezing point temperature (Davies, 2014), which poses a unique disadvantage for applications such as cell cryopreservation, as cells benefit from non-colligative freezing point depression but are susceptible to rapid ice expansion (Deller et al., 2014). To address these limitations, scientists and engineers have turned to bioinspired synthetic mimics as resilient alternatives to IBPs for material applications in non-physiological conditions.

Bioinspired synthetic IBP mimics

Synthetic molecules present a unique advantage over IBPs, as they offer tunable pendant moieties, architectures, and scalability for increasingly accessible ice growth mitigation technologies and improved robustness in non-physiological environments. Identifying new materials that mimic IBP function, such as IRI activity, is crucial for targeting niche engineering applications in non-physiological environments. Antifreeze glycoproteins (AFGPs), a subset of IBPs, are among the most commonly mimicked IBPs as they demonstrate potent IRI activity at low concentrations (He et al., 2018; Stubbs et al., 2019; Congdon et al., 2013, 2015; Mitchell et al., 2014, 2015; Biggs et al., 2017). For example, poly(vinyl alcohol) (PVA) has exhibited notable biomimetic antifreeze behavior (Congdon et al., 2013, 2015; Mitchell et al., 2014; Budke and Koop, 2006), is easy to produce, and has shown promise for multiple cryopreservation applications (Deller et al., 2014; Hasan et al., 2018; Mitchell et al., 2019). One study demonstrated that 27 kDa PVA

CellPress
OPEN ACCESS

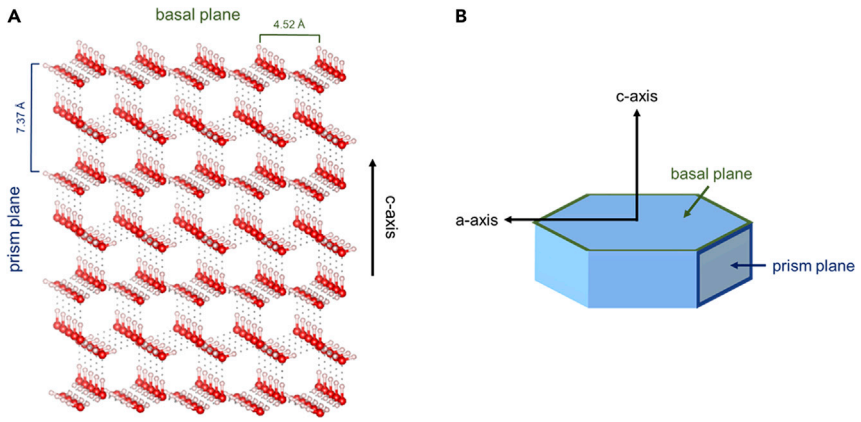

Figure 1. Schematic representations of hexagonal ice crystals

(A) Microscopic hexagonal ice demonstrating lattice constants for the basal plane and prism face. Figure was made using VESTA software (Momma and Izumi, 2011).

(B) Macroscopic hexagonal ice crystallite with basal plane and prism face.

exhibited IRI behavior at 0.05 mg mL^{-1} (1.6 μM) (Budke and Koop, 2006). Similarly, a study by the authors demonstrated that a 41.4 kDa poly(2-hydroxypropyl methacrylamide) (PHPMA) exhibited IRI behavior at 0.01 mg mL^{-1} (242 nM) (Delesky, 2020). Both PVA and PHPMA show IRI activity at concentrations comparable to the nanomolar concentrations in which native IBPs are active. Other molecules, such as pigments (Drori et al., 2016), polymer-modified nanoparticles (Stubbs et al., 2018), polyampholytes (Stubbs et al., 2017), quantum dots (Bai et al., 2017), and nanocelluloses (Li et al., 2019) also exhibit ice interactions similar to IBPs. While certain synthetic molecules with varying chemistries have proven effective in terms of mimicking the antifreeze behavior of IBPs, further investigation and intentional design of synthetic molecules with exceptional biomimetic antifreeze behavior in non-physiological environments would broaden possible applications in industry sectors that currently rely on anti-icing solutions with notable drawbacks.

Scope of review

This work presents a comprehensive review on the performance of IBPs and bioinspired synthetic mimics in non-physiological environments. First, ice interaction properties are described (thermal hysteresis, dynamic ice shaping, ice recrystallization inhibition, ice growth rate, and ice nucleation), and characterization techniques for each property are detailed. Next, a meta-analysis for IBP and synthetic analog performance in non-physiological environments is conducted, synthesizing data from literature to elucidate the influence of molecule and environment on ice interaction properties. Finally, this meta-analysis is used to illuminate and discuss broad trends, research gaps, persistent challenges, and opportunities for advancement of the field.

ICE INTERACTION PROPERTIES AND CHARACTERIZATION TECHNIQUES

Properties and physical characteristics of ice

To develop targeted mitigation strategies that prevent damage from ice growth, it is important to understand the properties and physical characteristics of ice. While ice is able to take on a variety of phases (Eisenberg and Kauzmann, 2005), the most common for standard temperatures and pressures is 1H hexagonal ice, which exhibits a hexagonal crystal with lattice constants of a = 4.52 Å along the basal plane and c = 7.37 Å along the prism plane (Eisenberg and Kauzmann, 2005). A microscopic crystallographic representation of 1H hexagonal ice with prominent basal and prism planes can be seen in Figure 1A, and a macroscopic representation of a hexagonal ice crystallite with prominent basal and prism planes is shown in Figure 1B.

Discussed below are methods used to investigate the interaction between materials and ice and how those materials influence ice formation and growth. Ice interactions include (1) thermal hysteresis, (2) dynamic ice shaping, (3) ice recrystallization inhibition, (4) ice growth rate, and (5) ice nucleation. Each ice interaction can typically be investigated using several techniques, resulting in either qualitative or quantitative data.

Thermal hysteresis (TH)

Thermal hysteresis (TH) is the non-colligative depression of the freezing point of solution while maintaining or elevating the melting point of solution, creating a temperature "gap" between freezing and melting temperatures. TH makes it difficult for solution to freeze (when the temperature is being lowered) and difficult for ice to melt (when the temperature is being elevated), providing a stable temperature range. TH is one metric used to measure the efficacy of IBPs to prevent ice growth within organisms, and is has previously been characterized as moderate (TH ~1°C) or hyperactive (TH ~5°C or more) (Davies, 2014; Dolev et al., 2016). TH was thought to be a unique property of IBPs until some synthetics were discovered to display marginal activity (TH < 1°C), such as zirconium acetate hydroxide (0.07°C) (Mizrahy et al., 2013), Safranine-O (0.6°C) (Drori et al., 2016), and glucose carbon dots (0.02°C) (Wang et al., 2020), although no synthetic has been able to match the TH activity of IBPs. TH can be measured through several means and is often reported as ΔT (°C), taken as the difference between the non-colligative freezing point depression and the non-colligative melting point elevation induced by the material. However, due to the lack of standardization, comparing TH activity among different labs and testing apparatus is imperfect. The reported TH activity can depend on the pause time before cooling starts, the size of the ice crystal, the rate of cooling, the solution composition, and the defined endpoint for low activity samples. For the sake of this review, values will be compared to provide an overview of an approximate range of activity.

Using osmometry to measure TH activity

The most common method for measuring TH is using a nanoliter osmometer. An aqueous sample is placed in immersion oil, frozen, and then slowly melted to achieve a single ice crystal, typically 10–50 μm in size. The temperature at which the single ice crystal is stable is taken as the melting point, and the single ice crystal is often incubated at that temperature for 5–15 min to facilitate interaction of the material with the ice crystal. The temperature is then lowered at a slow rate (~0.01°C min^{-1}) until ice growth is observed. The difference between the melting point temperature and the temperature of growth is taken as the TH (Braslavsky and Drori, 2013). A microfluidic cold finger has been developed that observes TH similar to the osmometer, allowing precise nucleation and control of the single ice crystal (Haleva et al., 2016).

Other methods to measure TH activity

While osmometry is the most common method, other techniques have been developed to measure the TH activity of materials. In a study performed by Inada and Lu (2004), a millimeter-size ice crystal was grown, hollowed out, exposed to solution, and then monitored for ice growth, yielding a similar TH gap as osmometry. Additionally, differential scanning calorimetry (DSC) has been used to observe TH by freezing the sample, then scanning for the melting point temperature. Once the melting point temperature is determined, the sample is frozen again, heated until just before the melting point, held for incubation, then frozen again to determine the TH based on the difference between the hold point temperature and the non-colligative freezing point temperature (Amornwittawat et al., 2008; DeVries et al., 2005; Lu et al., 2002). However, DSC is not used as frequently because supercooling can occur in the DSC sample pan, leading to unpredictable and unreproducible freezing points (Hill, 1991; Whale et al., 2015).

Dynamic ice shaping (DIS)

Dynamic ice shaping (DIS) is the reshaping of the 1H hexagonal ice structure by restricting growth in the plane of ice that the material is adsorbed to, and tends to be observed at concentrations lower than necessary for TH activity. For IBPs, the change in ice crystal geometry is indicative of the plane(s) of adsorption, and is sometimes observed when TH activity is not able to be measured. Bipyramidal ice is seen when the prism plane of ice is restricted, and hexagonal or "lemon"-shaped ice is seen when both the prism and basal planes of ice are restricted (Dolev et al., 2016). For materials other than IBPs, it has been shown that binding to the ice face is not required for ice growth inhibition, but changes in morphology are still seen. This is possibly due to material adsorption to the ice surface and preventing further ice growth through steric inhibition (Burkey et al., 2018). Often, DIS is observed through osmometry similar to TH although without determining a TH gap.

Ice recrystallization inhibition (IRI)

Ice recrystallization is the process through which larger ice crystals expand at the expense of smaller ice crystals, a phenomenon known as Ostwald ripening (Voets, 2017). Ice recrystallization inhibition (IRI) is the limitation of ice recrystallization through the Gibbs-Thompson effect. Several methods have been

established to determine the IRI activity of a material. The most common unit of reporting is percent mean largest grain size (% MLGS), which constitutes measuring ice grains along their longest axis and then normalizing the average size of the sample solution by the average grain size for the control solution tested, allowing comparison across solution type, and even test method. IRI activity ranges from negligible to moderate to potent. Negligible IRI activity is described by a large % MLGS (>∼80) that is often within error of control solution grain size, whereas potent IRI activity is described by a small % MLGS (<∼30), and moderate activity lies between negligible and potent. For preventing ice-induced damage, potent IRI activity is favored because it correlates with ice formation and growth inhibition. Similar to measuring TH activity, the reported values for IRI are imperfect as variations in methodology can influence the endpoint of the ice crystals. Some variables that can affect the growth are the temperature of the cold stage, the solution composition, and the endpoint of the assay. However, it is valuable to understand the range of IRI activity one might expect for an approximation of material performance.

Splat assays to measure IRI activity

The splat assay was established in 1986 by Knight and Dumani (1986). The splat assay creates a monolayer of polycrystalline ice by dropping a 10–20 μL droplet from ∼2 to 3 m onto a chilled glass slide, typically resting on top of an aluminum block that is chilled by dry ice. The glass slide with the ice monolayer is then transferred to a cold stage on a microscope and annealed at a sub-melting point temperature (approx. −6°C to −15°C) to monitor ice recrystallization over time. Wu et al. (2017) determined that the sub-melting point or annealing temperature for the splat assay plays a more critical role in ice grain size than nucleation temperature, and that larger ice grains will be seen with warmer annealing temperatures. Briefly, nucleation is the random formation of nascent crystals, and further described in Section Ice nucleation. The sample is often incubated at the annealing temperature for time intervals ranging from 30 min to 18 h, depending on the IRI activity of the molecule (*e.g.*, longer incubation periods are used for materials with more potent IRI activity). The data are reported either qualitatively by comparing micrographs at given time points or quantitatively by reporting % MLGS. It has been shown that deionized or ultrapure water will provide false positives, as any molecule in pure water will accumulate at the ice grain boundaries and prevent ice recrystallization (Knight et al., 1995). Thus, low concentrations of salt additives are necessary to keep the molecules at the solid-liquid interface, and active molecules will prevent ice recrystallization whereas inactive molecules will not.

Sucrose sandwich assays to measure IRI activity

The sucrose sandwich assay was developed by Worrall et al. (1998) but only became widely used after the method was validated by Budke and Koop (2006). The sucrose sandwich assay is performed by adding the material of interest to a sucrose solution (20%–40% sucrose) and sealing ≤1 μL of solution between two pieces of coverslip glass using silicone grease. The sandwich is flash frozen by exposing it to a temperature of −50°C or less to create a polycrystalline sample, then placed on a microscope cold stage (approx. −6°C to −15°C) and annealed between 1 and 18 h with monitoring at one or more time intervals. The data are reported similarly to the splat assay, as either qualitative micrographs or by quantitative % MLGS. The sucrose sandwich assay offers an advantage for monitoring solutions with insoluble components because the high percentage of sucrose prevents interference from insoluble particles. Additionally, quantitative analysis can be performed computationally for the sucrose sandwich assay due to the lack of grain impingement. However, the high percentage of sucrose in solution also slows the ice recrystallization process requiring longer annealing times to get an accurate comparison of material performance.

Other assays to measure IRI activity

One of the drawbacks for both the splat and sucrose sandwich assays is the time required to monitor the IRI activity of a single sample. A few techniques have been developed to improve the throughput of IRI testing; however, they have yet to be widely adopted. A capillary tube assay was developed by Tomczak et al. (2003). The capillary tube assay is performed by sealing samples in a 10 μL capillary tube (1 mm outer diameter) and snap freezing by placing into chilled 2,2,4-trimethylpentane (approx. −50°C by dry ice). The samples are then transferred to a jacketed beaker filled with the same solvent cooled to the annealing temperature. The capillary tube assay allows for multiple samples (∼15) to be viewed at once for side-by-side comparison and allows for long-term storage of the samples. However, the quality of image is reduced due to the curvature of the capillary tubes and direct grain counting is obscured. Thus, the capillary tube assay increases throughput but provides exclusively qualitative comparisons.

A high-throughput antifreeze protocol (HTAP) using a 96-well microtiter plate assay was developed by Gilbert et al. (2004). Samples are loaded into a 30% sucrose solution and compared to positive (IRI active) and negative (IRI inactive) controls. The plate is flash frozen at −70°C and held at temperature for 10 min, then placed on a cold stage to anneal for 5 days. Samples that remain frozen after annealing are said to be IRI active, while samples that melt are inactive. The HTAP method allows for high throughput of samples with a qualitative comparison; however, the 5-day incubation period is long and the protocol can lead to false positives.

A high-capacity endpoint device was developed by Graham et al. (2018) that allows up to 12 samples to be compared side-by-side. The endpoint device consists of a sapphire slide with 8–12 sample wells of about 45 μm diameter surrounded by a superhydrophobic coating. Samples of approximately 1 μL are loaded into the sample wells, and a slide with a fluorinated surface coating of trichloro(1,1,2H,2H-perfluorooctyl)silane is placed on top of the sample. The sample is then annealed and monitored for grain growth. The high-capacity device is able to produce high-quality images with a possibility for both qualitative and quantitative comparisons and can be washed with a detergent for repeated use. However, this method requires sapphire slides for high-quality images and a specially manufactured device making it potentially cost prohibitive compared to other IRI measurement methods. Finally, the superhydrophobic coating is sensitive to pH, so samples cannot be tested in some pH environments (*e.g.*, alkaline) using this method.

Ice growth rate

Ice growth rate investigates the change in ice crystal size, often along a specified ice crystal axis (*e.g.*, a-axis or c-axis, Figure 1B), over time at a set temperature below the freezing point of solution. Currently, there is no well-established method to measure rate of growth, but some experimental techniques have been developed (Mizrahy et al., 2013; Olijve et al., 2016; Huang et al., 2012). Of note, the rates and units often differ based on the method employed, which makes it difficult to directly compare results across methodologies. The reported values for ice-growth rate are additionally imperfect due to the variations in methodology. Some variables that can affect the growth are the temperature of the cold stage, the solution composition, and the resolution of the time points. Ice growth rate is more often used to investigate synthetic materials that do not stop the growth of ice, but instead slow it down. However, it is valuable to understand the range of ice growth rates one might expect for an approximation of material performance.

Osmometry to measure ice growth rate

Similar to measuring TH, osmometry can be used to determine ice growth by monitoring the growth of a singular ice crystal. A singular ice crystal is monitored for changes in diameter across either the a-axis or c-axis of ice, and is often reported as a unit of $\mu m\ sec^{-1}$ or $\mu m\ ms^{-1}$. Typically, multiple holding temperatures below the freezing point of solution will be used and expressed as Δ°C below freezing, and often performed in increments of 0.01 or 0.02°C. Rate determination using osmometry is sometimes used as a method to report TH activity for molecules with marginal TH, as rates less than $0.02\ \mu m\ s^{-1}$ are considered to be TH active (Mizrahy et al., 2013). Values are often reported as rate as a function of Δ°C, and tend to exhibit a sigmoidal curve.

Sucrose sandwich assays to measure ice growth rate

The sucrose sandwich assay described above in Section Sucrose sandwich assays to measure IRI activity is sometimes used to determine the rate of growth. Because the ice grains are well defined and do not undergo impingement, the sample can be monitored using a camera at multiple pre-determined time intervals to observe and quantify ice grain diameter over time. Ice growth rate measurements are often reported as $\mu m^2\ min^{-1}$ or $\mu m^3\ min^{-1}$. A circle Hough transform (CHT) algorithm has been developed to improve video processing to facilitate rapid analysis and material comparison (Olijve et al., 2016).

Silicon isolator method to measure ice growth rate

The silicon isolator method was developed by Huang et al. (2012) and is performed by sealing ≤20 μL of sample in silicon isolator wells between two glass slides and placed on a room temperature thermal microscope stage. The sample is then cooled and monitored for ice growth using a camera. The rate of growth is quantified by measuring the advancement of the ice crystal front over time, and reported as $\mu m\ sec^{-1}$.

CellPress
OPEN ACCESS

Table 1. Overview of experimental characterization techniques for ice interaction properties

	Measure of Performance				
Experimental Technique	TH	DIS	IRI	Rate of Growth	Ice Nucleation
Osmometry	✓	✓		✓	
mm Ice Crystals	✓				
Differential Scanning Calorimetry	✓				
Splat Assays			✓		
Sucrose Sandwich Assays			✓	✓	✓
Capillary Tube Assay			✓		
High-Throughput Antifreeze Protocol			✓		
High-Throughput Device Assay			✓		
Silicon Isolator Assay				✓	
%Droplets Frozen Assay					✓
Time until Nucleation Assay					✓

Filled and unfilled cells represent quantitative and qualitative measurements, respectively.

Ice nucleation

Some IBPs exhibit a property known as ice nucleation and readily enable the heterogeneous formation of ice crystals. Ice nucleation is useful for atmospheric science, specifically with regard to cloud formation (O'Sullivan et al., 2015, 2016; Hiranuma et al., 2019). At present, a singular method for determining ice nucleation efficacy has not been well established. However, two main methods of investigating ice nucleation have been reported: percentage of droplets frozen (Congdon et al., 2015; Biggs et al., 2017; Whale et al., 2015), and time until nucleation (Yang et al., 2016; He et al., 2016; Akhtar et al., 2019).

Percentage of droplets frozen to measure ice nucleation

An array of ~1 μL sample droplets is placed in wells or separated by a hydrophobic surface. The surface is then placed on a microscope cold stage set to ambient temperature (15–20°C) and monitored with a camera. The stage is cooled at a constant rate, normally from ambient temperature to −40°C to ensure a uniform and equilibrium cooling of the samples. Nucleation is reported as the percentage of droplets frozen at a given temperature, and most experiments are performed until 100% of samples have frozen (Congdon et al., 2015; Biggs et al., 2017; Whale et al., 2015).

Time until nucleation to measure ice nucleation

A drop of solution is placed in an isolated sample cell, often composed of a hydrophobic sealant (*e.g.*, a silicon o-ring) that is then positioned between two cover glass slips. Ice nucleation is measured by monitoring the time it takes for ice formation after the substrate equilibrates at a specific temperature, and the time until nucleation is reported in milliseconds or seconds (Yang et al., 2016; He et al., 2016).

An additional time until nucleation method was developed by Akhtar et al. (2019), where the ice prevention capabilities of hydrophobic surfaces were determined by dispensing ~4 μL of water onto the surface, lowering the temperature to a set holding temperature, and monitoring the time until freezing. Results are reported in milliseconds or seconds and describe the time until freezing at the holding temperature.

Table 1 provides an overview of experimental characterization techniques for determining ice interaction properties as well as resulting qualitative or quantitative resulting data. Depending on the measure of performance desired, Table 1 can help determine which experimental technique to employ. To understand all the ice interaction properties of a material, multiple techniques would have to be used.

EFFECT OF ENVIRONMENT ON ICE INTERACTION

According to available literature, physiological environments with a neutral (~7) pH and minimal solution additives (*e.g.*, salts, sugars) are the most common for investigating ice formation and growth. Non-physiological environments include those with deviations from neutral pH (pH $\leq$ 6, pH $\geq$ 8) or those with high

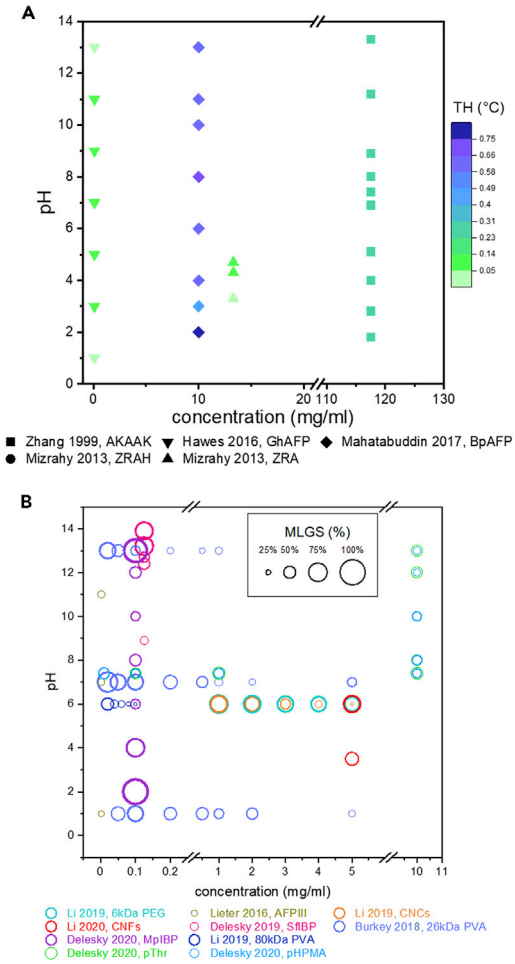

Figure 2. A review of material performance in pH adjusted environments (A) TH activity for several ice-binding proteins.(B) IRI activity for several ice-binding proteins and polymeric materials. The % MLGS is represented by circles, where larger diameters indicate larger % MLGS and lower IRI activity. Smaller diameter circles indicate small % MLGS and higher IRI activity (Delesky, 2020; Mizrahy et al., 2013; Burkey et al., 2018; Zhang and Laursen, 1999; Hawes, 2016; Mahatabuddin et al., 2017; Li et al., 2019, 2020; Leiter et al., 2016, 2018; Ren et al., 2019).

concentrations of solution additives (*e.g.*, salts and sugars). In this section, a meta-analysis of ice interaction properties of materials in non-physiological environments is presented.

Ice interaction properties in non-neutral pH environments

Some applications benefit from materials that can prevent ice growth in highly alkaline environments, such as portland cement concrete used in civil engineering, which has an internal pore solution pH of 13. Figures 2A and 2B show the limited data that are available to describe the effect of pH and concentration on TH and IRI activity, respectively, for different materials. In general, previous studies have measured TH activity with respect to altered environmental pH at one specific concentration. In contrast, IRI activity (% MLGS) has generally been measured in one specific environmental pH over a range of concentrations.

Figure 2A shows TH activity as it relates to concentration and environmental pH for different materials, with blue data points indicating higher TH activity. For AFPs from the species *Barfin plaice* (BpAFP) and *Gomphiocephalus hodgsoni* (GhAFP) and the AFP synthetic mimic (AKAAK), the environmental pH does not influence the TH activity. More specifically, as the pH increased from 1 to 13, the TH activity of BpAFP, GhAFP, and AKAAK remained relatively constant at 0.63 $\pm$ 0.10°C, 0.06 $\pm$ 0.01°C, and 0.24 $\pm$ 0.1°C, respectively (Zhang and Laursen, 1999; Hawes, 2016; Mahatabuddin et al., 2017). Finally, Mizrahy

et al. (2013) investigated zirconium acetate (ZRA), which requires slightly acidic pH to function due to the oligomerization of the material, seen as a higher TH (0.07°C) at a pH of 4.7.

Figure 2B shows IRI activity measured in % MLGS compared to the concentration and environmental pH for different materials. At pH 6–7, 26 kDa PVA shows moderate IRI activity (75% MLGS) at 0.05 mg mL^{-1}, whereas 80 kDa PVA shows potent IRI activity (20% MLGS) at 0.04 mg mL^{-1}, substantiating that there is a molecular weight dependence for some synthetic molecules (Li et al., 2019; Burkey et al., 2018). Additionally, 26 kDa PVA exhibits similar IRI activity at pH 1 and pH 13 when compared to pH 7, showing that PVA is resistant to changes in environmental pH (Burkey et al., 2018). Similarly, PHPMA exhibits similar IRI activity at pH 13 as it does at pH 7 (Delesky, 2020). Other synthetics (CNCs and CNFs) exhibit negligible efficacy in all pH environments investigated (Li et al., 2019, 2020). AFPIII maintained potent IRI at both acidic and alkaline pH (pH 1 and 11). However, extreme alkaline environments like those seen in concrete (≥ pH 13) have not been investigated (Leiter et al., 2016, 2018).[106] The proteins SfIBP and MpIBP were tested in alkaline pH greater than those conducted to AFPIII, and demonstrated that IRI activity was lost above pH 12.5. MpIBP and SfIBP were shown to denature in alkaline pH (pH > 10), but retained IRI activity (pH < 12.5), indicating that the pendant functional groups were sufficient to elicit IRI activity despite the loss of conformational structure (Delesky et al., 2019, 2020).

These data demonstrate significant gaps for TH and IRI efficacy in varied pH environments. To better understand the influence of pH on TH activity, more thorough investigations of the simultaneous effect of pH and concentration should be conducted, as all current studies only examine the effect of pH at a singular concentration. At present, only two IBPs are characterized for TH performance in varied pH environments. Additional IBP investigations have the potential to elucidate a trend with changes in pH. A few synthetic molecules have been shown to exhibit TH behavior in physiological environments (*e.g.*, safranine-O). Investigating TH performance under varied pH could demonstrate potential robust performance. Research on IRI activity of molecules in non-physiological environments would benefit from investigations in slightly acidic (3 < pH < 6) and slightly basic (8 < pH < 11) solutions, especially for concentrations <10 mg/mL. Additionally, given that a number of synthetic molecules that exhibit IRI activity in physiological solutions, investigating changes in IRI performance in varied pH environments offers the potential to further highlight the resiliency and efficacy of synthetic molecules compared to IBPs.

A few studies have investigated the effect of pH on ice growth rate. These data are summarized in Table 2. In general, active molecules exhibit slower growth rates in non-physiological, pH-adjusted environments compared to physiological environments, potentially due to the additional interference of pH adjustors on the hydrogen bonding network of ice. Burkey et al. (2018) determined that acidic environments increased the ice growth rate with added PVA, whereas basic environments reduced the ice growth rate with added PVA compared to pH 7 environments. Additionally, the authors demonstrated that 1 M NaOH reduced the rate of growth for polymers without IRI activity (PEG, atactic PG, and isotactic PG) compared to 1 M NaCl. Mizrahy et al. (2013) looked at ZRA and ZRAH, small molecules that require acidic pH of ~4.7 to promote active oligomeric species in solution, and determined that a pH of 4.7 resulted in the slowest ice growth rate. The effect of non-neutral environmental pH on ice nucleation has not yet been investigated, representing an opportunity for future research.

Ice interaction properties in the presence of ionic additives

Within organisms, IBPs typically work synergistically with other internal constituents to prevent ice formation or to regulate ice growth. For use in non-physiological environments, understanding the synergy between IBPs and controlled additives is important for tuning ice formation or ice growth within an engineered system. Salt or other ionic constituents are common additive to enhance TH activity. A summary of the influence of salt additives on TH activity is shown in Figure 3.

According to the data presented in Figure 3, salt additives appear to enhance the TH activity of hyperactive proteins Amornwittawat et al. (2008); Kristiansen et al. (2008); Li et al. (1998); Liu et al. (2015) more than moderately active proteins (Evans et al., 2007). In general, the synergy between salt additives and IBPs follows the Hofmiester series. However, a few notable exceptions exist. First, the IBPs demonstrate a stronger-than-anticipated synergy with zinc chloride, sodium nitrate, sodium iodide, and cobalt chloride. Second, the IBPs show a dependence on salt concentration for ammonium bicarbonate, which induced

Table 2. The influence of environmental pH on the ice growth rate

Paper	Environment	Material	Concentration	ΔT [°C]	Rate
Mizrahy et al. (2013)	–	buffer	–	0.022	2.63 μm s^{-1}
	pH 3.3	ZRAH	150 mM	0.022	2.13 μm s^{-1}
		ZRA	150 mM	0.02	0.076 μm s^{-1}
	pH 4.2	ZRAH	150 mM	0.022	0.11 μm s^{-1}
		ZRA	150 mM	0.025	0.012 μm s^{-1}
	pH 4.7	ZRAH	150 mM	0.022	0.01 μm s^{-1}
		ZRA	150 mM	0.025	0.009 μm s^{-1}
Burkey et al. (2018)	0.1 M HCl(pH 1)	–	–	–	27.2 μm^3 min^{-1}
		26 kDa PVA	0.5 mg mL^{-1}	–	15.3 μm^3 min^{-1}
			5 mg mL^{-1}	–	0.6 μm^3 min^{-1}
	0.1 M NaCl (pH 7)	–	–	–	23.3 μm^3 min^{-1}
		26 kDa PVA	0.5 mg mL^{-1}	–	8.9 μm^3 min^{-1}
			5 mg mL^{-1}	–	0.3 μm^3 min^{-1}
	0.1 M NaOH (pH 13)	–	–	–	31.9 μm^3 min^{-1}
		26 kDa PVA	0.5 mg mL^{-1}	–	0.04 μm^3 min^{-1}
			5 mg mL^{-1}	–	0.1 μm^3 min^{-1}
	1 M NaOH	PEG	50 mg mL^{-1}	–	7.0 μm^3 min^{-1}
		PG - atactic	50 mg mL^{-1}	–	25.7 μm^3 min^{-1}
		PG - isotactic	50 mg mL^{-1}	–	29.8 μm^3 min^{-1}

more synergy at high concentrations (0.5 M) than at low concentrations (0.2 M). Further investigations are required to understand the deviant synergy between the salt additives and IBPs, which could possibly be attributed to salt concentration, IBP concentration, or IBP type. Finally, there is a contradictory contribution by ammonium sulfate, suggested by the high synergy with the IBP RiAFP, but minimal synergy with the IBP DcAFP (Figure 3), which may be due to specific protein interactions. To date, no studies have been performed to investigate synergistic effects between salts and synthetic materials to enhance TH activity, again representing an opportunity for future research.

Limited studies have investigated the synergistic effects that salt additives have on IRI activity. Leiter et al. (2016) investigated AFPIII under the influence of increasing concentrations of NaCl and found that IRI activity of AFPIII increased as the salt concentration increased. Surís-Valls et al. (115) also investigated the IRI activity of two types of AFGP under the influence of 0.1 M salt additives (NaCl, $Na_3C_6H_5O_7$, $Na_2[B_4O_5(OH)_4]$, $NaNO_3$, and Na_3PO_4) and found that all salt additives improved the IRI activity of the AFGPs. Balcerzak et al. (2013) demonstrated that LiCl and KCl reduced the IRI activity of moderately active carbohydrate molecules based on AFGPs. Wu et al. (2017) showed that salt additives affect the final crystal size for control salt solutions based on the Hofmeister series but did not demonstrate synergistic effects with IRI active materials. In general, the Hofmeister series seems to effect the recrystallization of ice, though further studies are required to fully elucidate potential synergistic effects for engineering applications. Only one study performed by the authors looked at the influence of salt additives on the IRI activity of synthetic materials. In that study, it was found that the addition of 151 mM salts with multivalent metallic cations ($CaCl_2$, $MgCl_2$, $CuCl_2$, and $AlCl_3$) reduced the IRI activity of 41.4 kDa pHPMA and eliminated the IRI activity of a 7.6 kDa polythreonine (Delesky, 2020).

The influence of ionic additives on ice growth rate of select IBPs and synthetic molecules has been studied (Table 3). To date, the effect of salt additives on ice nucleation, however, has not yet been investigated. Suris-Valls and Voets. (2019) investigated two types of AFGPs and found that all salt additives reduced the rate of growth of the AFGPs in accordance to the Hofmeister series. Burkey et al. (2018) studied 26 kDa PVA and assessed how 0.1 M salts (NaCl, NaSCN, and LiCl) affected the ice growth rate, determining that both NaSCN and LiCl reduced the rate of growth by 64% and 97% compared to NaCl, respectively. While more data are required to definitively determine the contribution of salt additives, it is likely that synergy may follow the Hofmeister series.

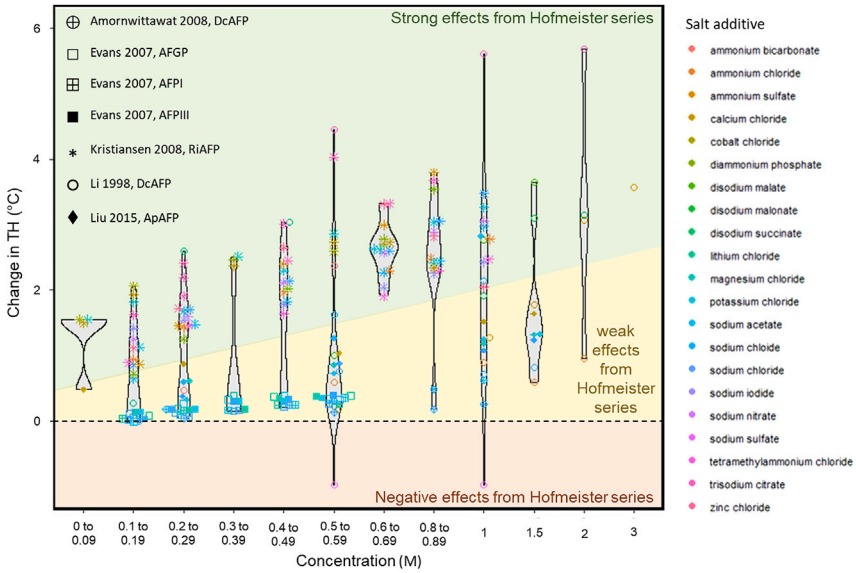

Figure 3. The effect of salt additives on TH activity, with synergistic contributions generally following the Hofmeister series

See (Amornwittawat et al., 2008; Kristiansen et al., 2008; Evans et al., 2007; Li et al., 1998; Liu et al., 2015).

Ice interaction properties in the presence of non-ionic additives

Similar to salts, non-ionic additives can behave synergistically with IBPs and synthetic materials to prevent or control ice formation and growth. As an example of non-ionic additives, small molecule polyols are often used as cryopreservation agents; however, some polyols can be toxic to cells upon thawing. Additionally, polyols are often used for plane deicers. Excess deicer can contaminate water runoff and the nearby environment (Kent et al., 1999). Materials that exhibit synergistic effects to reduce ice formation and growth could reduce the amount of toxic polyols utilized while retaining adequate prevention of ice growth.

The non-ionic additives reported in the literature and analyzed herein fell into three main categories: sugars (or rings with pendant hydroxyls), linear hydroxyl-containing molecules, and carboxylated molecules. The effects of these additives on TH activity are shown in Figure 4.

As shown in Figure 4, most non-ionic additives act synergistically to improve the TH activity of IBPs as indicated by the positive increase of TH activity with the increase of additive concentration. In general, as the concentration of non-ionic additive increased ($\geq$1 M), there was a corresponding improvement in TH activity. Notably, carboxylated molecules as a non-ionic additive demonstrated the greatest synergy with respect to concentration as there was a greater increase of TH activity (Figure 4C) at the same concentration of additive compared to sugars (Figure 4A) and hydroxyl-containing molecules (Figure 4B). In addition, some studies have investigated the synergistic effect of larger molecules as non-ionic additives, such as proteins or polymers, on TH activity. For example, Funakoshi et al. (2008) examined the effect of adding a 10 kDa polymer, ammonium polyacrylate (NH_4PA), on the TH activity of AFPI and reported that 66 mg mL^{-1} NH_4PA increased TH by ~360%, and 167 mg mL^{-1} NH_4PA increased TH by ~460%. Berger et al. (2019) demonstrated that a passive isoform of AFPIII (*i.e.*, no TH activity) would enhance the TH activity of active isoforms. Wu and Duman (1991) and Wang and Duman (2006) demonstrated that the introduction of other components of insect hemolymph increases TH activity, further substantiating that adding synergistic components can improve protein efficacy. Despite the literature available on IBPs, no studies have investigated synergistic effects between non-ionic additives and synthetic materials to enhance TH activity, which represents another future research opportunity.

Limited studies have investigated the influence of non-ionic additives on IRI activity. No studies to date have examined the effect on ice growth rate or ice nucleation. Ishibe et al. (2019) demonstrated the IRI activity of PVA could be improved by adding non-ionic molecules that do not demonstrate IRI activity. Molecules that worked were: 4kDa PEG, lactose (>10 mg mL^{-1}), 12kDa poly acrylic acid, 7.7 kDa

Table 3. The influence of ionic additives on ice growth rate

Reference	Environment	Material	Concentration	Rate [μm^3 min^{-1}]
Suris-Valls and Voets (2019)	30 wt% sucrose	AFGP1-5	5 nM	0.67
		AFPIII rQAE	500 nM	1.03
	+0.1 M $NaNO_3$	AFGP1-5	5 nM	0.48
		AFPIII rQAE	500 nM	0.93
	+0.1 M NaCl	AFGP1-5	5 nM	0.45
		AFPIII rQAE	500 nM	0.42
	+0.1 M $Na_2[B_4O_5(OH)_4]$	AFGP1-5	5 nM	0.59
		AFPIII rQAE	500 nM	0.36
	+0.1 M Na_3PO_4	AFGP1-5	5 nM	0.26
		AFPIII rQAE	500 nM	0.29
	+0.1 M $Na_3C_6H_5O_7$	AFGP1-5	5 nM	0.01
		AFPIII rQAE	500 nM	0.24
Burkey et al. (2018)	0.1 M NaCl	–	–	23.3
		26 kDa PVA	0.5 mg mL^{-1}	8.9
			5 mg mL^{-1}	0.3
	1 M NaCl	PEG	50 mg mL^{-1}	49.2
		PG - atactic	50 mg mL^{-1}	71.9
		PG - isotactic	50 mg mL^{-1}	90
	0.1 M NaSCN	–	–	24.6
		26 kDa PVA	0.5 mg mL^{-1}	3.2
			5 mg mL^{-1}	0.2
	0.1 M LiCl	–	–	20
		26 kDa PVA	0.5 mg mL^{-1}	0.2
			5 mg mL^{-1}	0.1

polymethacrylate, and 1.3 kDa poly(vinyl prylodine) (Ishibe et al., 2019). Molecules that did not work include ethylene glycol, glucose, lactose (<10 mg mL^{-1}), acrylic acid, methacrylate, and 15kDa poly(vinyl prylodine). The authors expect that the depletion forces incurred by additional soluble polymers were somehow necessary to facilitate interactions between the IRI-active PVA and ice (Ishibe et al., 2019).

CONCLUDING REMARKS AND FUTURE DIRECTIONS

IBPs and their synthetic mimics offer a potentially disruptive route to engineer novel ice growth mitigation material technologies for non-physiological engineering applications. Given that ice forms in most water-containing systems, understanding material performance outside of physiological environments is a crucial next step toward implementing IBPs and synthetic mimics in real-world engineering applications.

Herein, we have reviewed the performance of IBPs and synthetic mimics in non-physiological environments. We addressed common methods for measuring ice interactions, as well as the change in material performance in non-neutral environments. The recent interest in identifying new, robust synthetic IBP mimics will broaden opportunities for new engineering applications. New, bioinspired molecular designs continue to increase synthetic molecule performance. We anticipate that a continued interdisciplinary approach to materials design and further investigations on synergy for complex engineering systems will improve IBP and synthetic mimic technology and expand their applications in a variety of fields.

We offer the following concluding remarks and insights into future directions for materials scientists in the field of IBPs and synthetic mimics:

1. The TH activity of IBPs can be tuned to achieve desired performance. Data from the literature show that the performance of IBPs can be tuned to target specific TH activities. TH activity can be tuned by adding repeats of existing amino acid sequences to enlarge the IBP, creating larger

CellPress
OPEN ACCESS

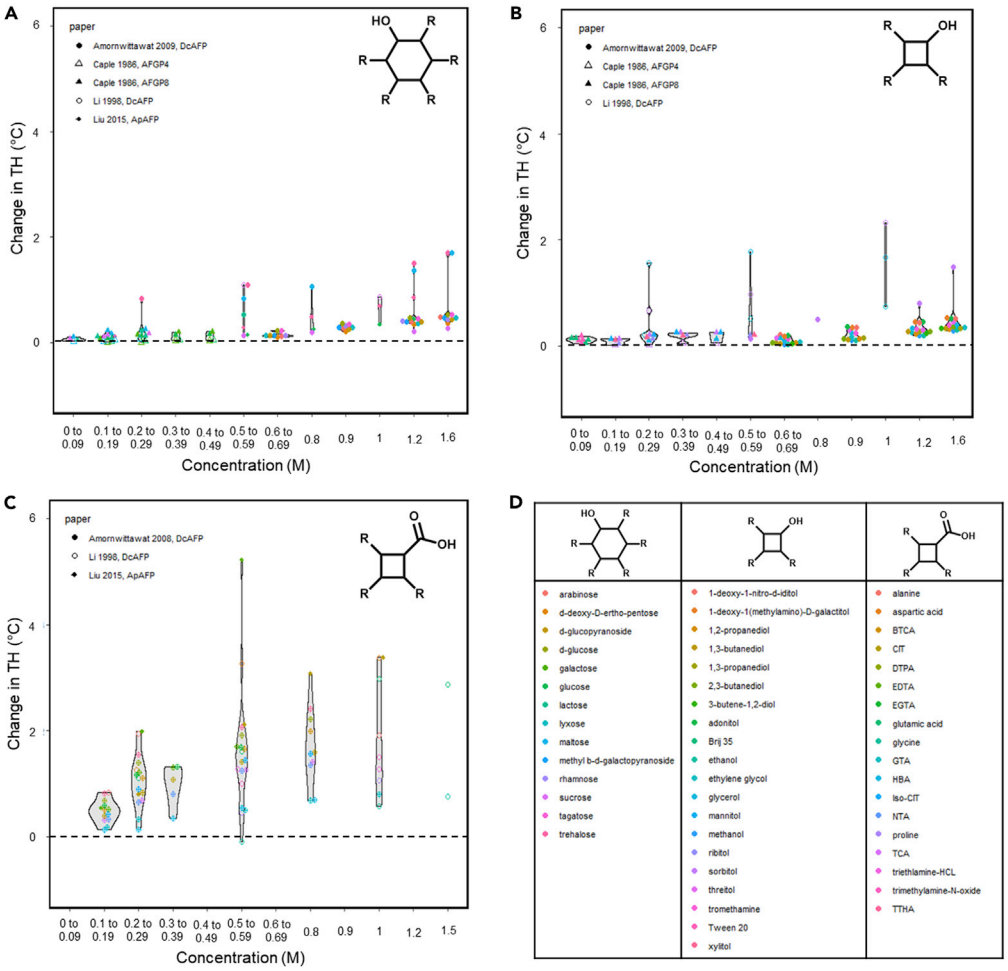

Figure 4. The effect of non-ionic additives on the change in TH activity for different AFPs

(A) Molecules with a sugar ring with at least one pendant –OH group. (B) Molecules with a linear or branched backbone (represented by a square) with at least one pendant –OH group.

(C) Molecules with a linear or branched backbone (represented by a square) with at least one pendant –COOH group.

(D) Table of materials reviewed in (a), (b), and (c), respectively. R groups could be a pendant –OH or other pendant functionalities (Amornwittawat et al., 2008, 2009; Li et al., 1998; Liu et al., 2015; Caple et al., 1986).

IBP conjugates using a polymeric linker, or adding synergistic constituents to bolster TH performance.

2. The external environment has a significant effect on IBP performance. In addition to altering IBPs on a molecular level, solution constituents have been shown to enhance IBPs performance. Non-active proteins, salt additives that follow the Hofmeister series and small hydrophilic molecules, such as sugars, hydroxyl-containing molecules, or carboxyl-containing molecules, behave synergistically with IBPs to mitigate ice growth. For IBPs, limited data indicate that these trends appear true for IRI activity as well. Overall, IBPs show significant promise for enhancing IBP performance with certain salts and small molecules, which may be beneficial for applications such as cryogenic fluids in aerospace applications, where small molecules with pendant hydroxyls are already used. Further investigations should focus on elucidating the synergies between IBPs and the solution chemistry for increasing IRI activity, reducing ice growth rate, and delaying ice nucleation.

3. Peptoids offer a promising synthetic route to approach the efficacy of IBPs for ice growth mitigation. Peptoids have demonstrated particularly promising TH and IRI activities, mimicking the functionalities of IBPs without requiring protein folding to function. Peptoids additionally offer more accessible scale-up with one-pot syntheses. Sequence-defined synthetic polymers, such as peptoids, offer

enhanced thermal and chemical stability in addition to a tunable structure and are more readily produced than folded proteins. The design and synthesis of peptoids provides a robust route for targeted, high-activity mimics of IBPs with the potential for increased control of the material structure for higher throughput materials with targeted TH and IRI activity. However, to date, the TH activity of remains in the marginally active category, and further research may yield peptoids in the moderate to hyperactive categories. Additionally, the field would benefit from further peptoid investigations based on structure, moieties, and size, as well as investigating the effects of non-physiological environments on activity.

4. Lower cost, bioinspired synthetic mimics offer improved stability and IRI activity performance in a wide range of solution chemistries but do not exhibit comparable TH activities of native IBPs. While the IRI activity of IBPs is still effective at concentrations several magnitudes lower than synthetic IBP mimics, the up-scalability and availability of synthetic production suggests promise and potential for engineering and other applications, especially for well-studied and readily available engineering polymers such as PVA. Unfortunately, drawing meaningful conclusions from disparate investigations of synthetic IBP mimics is difficult due to the lack of uniformity of testing conditions, and is further confounded by the inherent variability in polymer systems, including molecular weight, polydispersity index, tacticity, and sometimes even degrees of substitution of pendant functional groups. While many of these variables have been investigated independently for specific polymer systems, no one conclusion can be drawn for the entirety of synthetic mimics.

While synthetic materials still require deeper understanding for their mechanism of action for suppressing ice growth, they could offer better alternatives for engineering applications in aggressive environments. To date, however, synthetic mimics have not been investigated thoroughly. Data from the literature show that the performance of synthetic IBP mimics can be tuned by molecular weight and pendant moieties, but there is limited data on the effects of solution composition. The limited data available today, however, suggest that IBP mimics exhibit promising activity under environmental stressors. Future investigations that determine the importance of salts, small molecules, and pH could highlight the potential of synthetic IBP mimics to provide revolutionary ice mitigation strategies for a variety of engineering applications. Additionally, further investigations detailing the effects of various pendant moieties could elucidate promising new polymer architectures that are more effective at mimicking the activities of native IBPs.

For example, self-assembled molecules, such as those shown by Drori et al. (2016) and Xue et al. (2019), demonstrated functional group spacing similar to IBPs, lending to increased material performance. However, self-assembling molecules have not yet been tested for resilience and IRI activity in non-physiological environments with complex solution chemistries. Additionally, other self-assembling molecules, such as liquid crystals, have controllable structure and spacing, potentially offering a dynamic system that could be tuned to exhibit a targeted TH or IRI activity based on molecule type or environmental conditions.

5. A proven mechanism of action for synthetic IBP mimics does not yet exist, which represents a significant—if not the primary—challenge for the field. While a paucity of molecular dynamics studies have been performed (Naullage et al., 2017; Naullage and Molinero, 2020), further molecular dynamics studies could be employed to further delve into and discover the mechanism(s) of action for synthetic molecules with regard to IRI activity, ice growth rate, and potential ice nucleation. Additionally, validation of the results from molecular dynamics simulations with experiments is still needed to elucidate a universal mechanistic theory of ice interaction. Understanding the mechanisms of action of IBPs and synthetic IBP mimics will ultimately improve the capacity for experimental design to target architectures that would better mitigate ice growth.

ACKNOWLEDGMENTS

This research was made possible by the Department of Civil, Environmental, and Architectural Engineering, the College of Engineering and Applied Sciences, and the Living Materials Lab at the University of Colorado Boulder with financial support from the United States (US) National Science Foundation (Award No. CMMI-1727788) and the National Science Foundation Graduate Research Fellowship Program. This work represents the views of the authors and not necessarily those of the sponsors.

AUTHOR CONTRIBUTIONS

Data curation, E.A.D.; formal analysis, E.A.D.; funding acquisition, W.V.S.III; investigation, E.A.D.; supervision, W.V.S.III; writing–original draft, E.A.D.; writing–review & editing, W.V.S.III. All authors have read and agreed to the published version of the manuscript.

DECLARATION OF INTERESTS

WVS is a founder of Prometheus Materials, Aureus Earth, and Minus Materials and a member of their scientific advisory boards. EAD and WVS are listed inventors of a related United States Patent PCT/US2020/038198.

INCLUSION AND DIVERSITY

One or more of the authors of this paper self-identifies as a member of the LGBTQ + community.

REFERENCES

Akhtar, N., Anemone, G., Farias, D., and Holst, B. (2019). Fluorinated graphene provides long lasting ice inhibition in high humidity. Carbon *141*, 451–456. https://doi.org/10.1016/j.carbon.2018.09.008.

Amornwittawat, N., Wang, S., Duman, J.G., and Wen, X. (2008). Polycarboxylates enhance beetle antifreeze protein activity. Biochim. Biophys. Acta Protein Proteomics *1784*, 1942–1948. https://doi.org/10.1016/j.bbapap.2008.06.003.

Amornwittawat, N., Wang, S., Banatlao, J., Chung, M., Velasco, E., Duman, J.G., and Wen, X. (2009). Effects of polyhydroxy compounds on beetle antifreeze protein activity. Biochim. Biophys. Acta Protein Proteomics *1794*, 341–346. https://doi.org/10.1016/j.bbapap.2008.10.011.

Arakawa, T., Prestrelski, S.J., Kenney, W.C., and Carpenter, J.F. (2001). Estabilidad de proteínas. Adv. Drug Deliv. Rev. *46*, 1–8.

Baardsnes, J., and Davies, P.L. (2002). Contribution of hydrophobic residues to ice binding by fish type III antifreeze protein. Biochim. Biophys. Acta Protein Proteomics *1601*, 49–54. https://doi.org/10.1016/S1570-9639(02)00431-4.

Baardsnes, J., Kondejewski, L.H., Hodges, R.S., Chao, H., Kay, C., and Davies, P.L. (1999). New ice-binding face for type I antifreeze protein. FEBS Lett. *463*, 87–91. https://doi.org/10.1016/S0014-5793(99)01588-4.

Bai, G., Song, Z., Geng, H., Gao, D., Liu, K., Wu, S., Rao, W., Guo, L., and Wang, J. (2017). Oxidized quasi-carbon nitride quantum dots inhibit ice growth. Adv. Mater. *29*, 1606843. https://doi.org/10.1002/adma.201606843.

Balcerzak, A.K., Febbraro, M., and Ben, R.N. (2013). The importance of hydrophobic moieties in ice recrystallization inhibitors. RSC Adv. *3*, 3232–3236. https://doi.org/10.1039/c3ra23220d.

Berger, T., Meister, K., Devries, A.L., Eves, R., Davies, P.L., and Drori, R. (2019). Synergy between antifreeze proteins is driven by complementary ice-binding. J. Am. Chem. Soc. *141*, 19144–19150. https://doi.org/10.1021/jacs.9b10905.

Biggs, C.I., Bailey, T.L., Graham, B., Stubbs, C., Fayter, A., and Gibson, M.I. (2017). Polymer mimics of biomacromolecular antifreezes. Nat. Commun. *8*, 1546. https://doi.org/10.1038/s41467-017-01421-7.

Braslavsky, I., and Drori, R. (2013). LabVIEW-operated novel nanoliter osmometer for ice binding protein investigations. J. Vis. Exp. e4189. https://doi.org/10.3791/4189.

Budke, C., and Koop, T. (2006). Ice recrystallization inhibition and molecular recognition of ice faces by poly(vinyl alcohol). ChemPhysChem *7*, 2601–2606. https://doi.org/10.1002/cphc.200600533.

Burkey, A.A., Riley, C.L., Wang, L.K., Hatridge, T.A., and Lynd, N.A. (2018). Understanding poly(vinyl alcohol)-mediated ice recrystallization inhibition through ice adsorption measurement and pH effects. Biomacromolecules *19*, 248–255. https://doi.org/10.1021/acs.biomac.7b01502.

Caple, G., Kerr, W.L., Burcham, T.S., Osuga, D.T., Yeh, Y., and Feeney, R.E. (1986). Superadditive effects in mixtures of fish antifreeze glycoproteins and polyalcohols or surfactants. J. Colloid Interface Sci. *111*, 299–304. https://doi.org/10.1016/0021-9797(86)90036-6.

Chakraborty, S., and Jana, B. (2018). Optimum number of anchored clathrate water and its instantaneous fluctuations dictate ice plane recognition specificities of insect antifreeze protein. J. Phys. Chem. B *122*, 3056–3067. https://doi.org/10.1021/acs.jpcb.8b00548.

Congdon, T., Notman, R., and Gibson, M.I. (2013). Antifreeze (Glyco)protein mimetic behavior of poly(vinyl alcohol): detailed structure ice recrystallization inhibition activity study. Biomacromolecules *14*, 1578–1586. https://doi.org/10.1021/bm400217j.

Congdon, T., Dean, B.T., Kasperczak-Wright, J., Biggs, C.I., Notman, R., and Gibson, M.I. (2015). Probing the biomimetic ice nucleation inhibition activity of poly(vinyl alcohol) and comparison to synthetic and biological polymers. Biomacromolecules *16*, 2820–2826. https://doi.org/10.1021/acs.biomac.5b00774.

Costantino, H.R., and Pikal, M.J. (2004). Lyophilization of Biopharmaceuticals, 2nd ed. (Springer Science & Business Media).

Davies, P.L., Hew, C.L., and Fletcher, G.L. (1988). Fish antifreeze proteins: physiology and evolutionary biology. Can. J. Zool. *66*, 2611–2617. https://doi.org/10.1139/z88-385.

Davies, P.L. (2014). Ice-binding proteins: a remarkable diversity of structures for stopping and starting ice growth. Trends Biochem. Sci. *39*, 548–555. https://doi.org/10.1016/j.tibs.2014.09.005.

Delesky, E.A., Frazier, S.D., Wallat, J.D., Bannister, K.L., Heveran, C.M., and Srubar, W.V. (2019). Ice-binding protein from Shewanella frigidimarinas inhibits ice crystal growth in highly alkaline solutions. Polymers (Basel) *11*, 299. https://doi.org/10.3390/polym11020299.

Delesky, E.A., Thomas, P.E., Charrier, M., Cameron, J.C., and Srubar, W.V. (2020). Effect of pH on the activity of ice-binding protein from Marinomonas primoryensis. Extremophiles *25*, 1–13. https://doi.org/10.1007/s00792-020-01206-9.

Delesky, E.A. (2020). Ice Recrystallization Inhibition of Ice-Binding Proteins and Bioinspired Synthetic Mimics in Non-Physiological Environments. Doctoral Dissertation (University of Colorado Boulder).

Deller, R.C., Vatish, M., Mitchell, D.A., and Gibson, M.I. (2014). Synthetic polymers enable non-vitreous cellular cryopreservation by reducing ice crystal growth during thawing. Nat. Commun. *5*, 3244–3247. https://doi.org/10.1038/ncomms4244.

Deluca, C.I., Davies, P.L., Ye, Q., and Jia, Z. (1998). The effects of steric mutations on the structure of type III antifreeze protein and its interaction with ice. J. Mol. Biol. *275*, 515–525. https://doi.org/10.1006/jmbi.1997.1482.

Ramløv, H., DeVries, A.L., Wilson, P.W., and Champaign, U. (2005). Antifreeze glycoproteins from the antarctic fish Dissostichus mawsoni studied by differential scanning calorimetry (DSC) in combination with nanolitre osmometry. Cryo-Letters *26*, 73–84.

DeVries, A.L. (1988). The role of antifreeze glycopeptides and peptides in the freezing avoidance of antarctic fishes. Comp. Biochem. Physiol. B Biochem. *90*, 611–621. https://doi.org/10.1016/0305-0491(88)90302-1.

Bar Dolev, M., Braslavsky, I., and Davies, P.L. (2016). Ice-binding proteins and their function.

Annu. Rev. Biochem. *85*, 515–542. https://doi.org/10.1146/annurev-biochem-060815-014546.

Drori, R., Li, C., Hu, C., Raiteri, P., Rohl, A.L., Ward, M.D., and Kahr, B. (2016). A supramolecular ice growth inhibitor. J. Am. Chem. Soc. *138*, 13396–13401. https://doi.org/10.1021/jacs.6b08267.

Duman, J.G., Bennett, V., Sformo, T., Hochstrasser, R., and Barnes, B.M. (2004). Antifreeze proteins in Alaskan insects and spiders. J. Insect Physiol. *50*, 259–266. https://doi.org/10.1016/j.jinsphys.2003.12.003.

Duman, J.G., and Olsen, T.M. (1993). Thermal hysteresis protein activity in bacteria, fungi, and phylogenetically diverse plants. Cryobiology *30*, 322–328. https://doi.org/10.1006/cryo.1993.1031.

Eisenberg, D., and Kauzmann, W. (2005). The Structure and Properties of Water (Oxford University Press on Demand).

Evans, R.P., Hobbs, R.S., Goddard, S.V., and Fletcher, G.L. (2007). The importance of dissolved salts to the in vivo efficacy of antifreeze proteins. Comp. Biochem. Physiol. Mol. Integr. Physiol. *148*, 556–561. https://doi.org/10.1016/j.cbpa.2007.07.005.

Fletcher, G.L., King, M.J., and Kao, M.H. (1987). Low temperature regulation of antifreeze glycopeptide levels in Atlantic cod (Gadus morhua). Can. J. Zool. *65*, 227–233. https://doi.org/10.1139/z87-037.

Frazier, S.D., Matar, M.G., Osio-Norgaard, J., Aday, A.N., Delesky, E.A., and Srubar, W.V. (2020). Inhibiting freeze-thaw damage in cement paste and concrete by mimicking nature's antifreeze. Cell Rep. Phys. Sci. *1*, 100060. https://doi.org/10.1016/j.xcrp.2020.100060.

Funakoshi, K., Inada, T., Kawabata, H., and Tomita, T. (2008). Cooperative function of ammonium polyacrylate with antifreeze protein type I. Biomacromolecules *9*, 3150–3156. https://doi.org/10.1021/bm800739s.

Gao, D., and Critser, J.K. (2000). Mechanisms of cryoinjury in living cells. ILAR J. *41*, 187–196. https://doi.org/10.1093/ilar.41.4.187.

Garnham, C.P., Gilbert, J.A., Hartman, C.P., Campbell, R.L., Laybourn-Parry, J., and Davies, P.L. (2008). A Ca2+-dependent bacterial antifreeze protein domain has a novel β-helical ice-binding fold. Biochem. J. *411*, 171–180. https://doi.org/10.1042/BJ20071372.

Garnham, C.P., Campbell, R.L., and Davies, P.L. (2011). Anchored clathrate waters bind antifreeze proteins to ice. Proc. Natl. Acad. Sci. U S A *108*, 7363–7367. https://doi.org/10.1073/pnas.1100429108.

Gilbert, J.A., Hill, P.J., Dodd, C.E.R., and Laybourn-Parry, J. (2004). Demonstration of antifreeze protein activity in Antarctic lake bacteria. Microbiology *150*, 171–180. https://doi.org/10.1099/mic.0.26610-0.

Grabowska, J., Kuffel, A., and Zielkiewicz, J. (2018). Molecular dynamics study on the role of solvation water in the adsorption of hyperactive AFP to the ice surface. Phys. Chem. Chem. Phys. *20*, 25365–25376. https://doi.org/10.1039/C8CP05027A.

Graether, S.P., Kuiper, M.J., Gagné, S.M., Walker, V.K., Jia, Z., Sykes, B.D., and Davies, P.L. (2000). β-Helix structure and ice-binding properties of a hyperactive antifreeze protein from an insect. Nature *406*, 325–328. https://doi.org/10.1038/35018610.

Graham, L.A., Agrawal, P., Oleschuk, R.D., and Davies, P.L. (2018). High-capacity ice-recrystallization endpoint assay employing superhydrophobic coatings that is equivalent to the 'splat' assay. Cryobiology *81*, 138–144. https://doi.org/10.1016/j.cryobiol.2018.01.011.

Graham, L.A., and Davies, P.L. (2005). Glycine-rich antifreeze proteins from snow fleas. Science *310*, 461. https://doi.org/10.1126/science.1115145.

Griffith, M., Ala, P., Yang, D.S.C., Hon, W.C., and Moffatt, B.A. (1992). Antifreeze protein produced endogenously in winter rye leaves. Plant Physiol. *100*, 593–596. https://doi.org/10.1104/pp.100.2.593.

Haleva, L., Celik, Y., Bar-Dolev, M., Pertaya-Braun, N., Kaner, A., Davies, P., and Braslavsky, I. (2016). Microfluidic cold-finger device for the investigation of ice-binding proteins. Biophys. J. *111*, 1143–1150. https://doi.org/10.1016/j.bpj.2016.08.003.

Harding, K. (2004). Genetic integrity of cryopreserved plant cells: a review. Cryo-Letters *25*, 3–22.

Hasan, M., Fayter, A.E.R., and Gibson, M.I. (2018). Ice recrystallization inhibiting polymers enable glycerol-free cryopreservation of microorganisms. Biomacromolecules *19*, 3371–3376. https://doi.org/10.1021/acs.biomac.8b00660.

Hawes, T.C. (2016). A root bond between ice and antifreeze protein. Cryobiology *73*, 147–151. https://doi.org/10.1016/j.cryobiol.2016.08.007.

Haymet, A.D.J., Ward, L.G., Harding, M.M., and Knight, C.A. (1998). Valine substituted winter flounder 'antifreeze': preservation of ice growth hysteresis. FEBS Lett. *430*, 301–306. https://doi.org/10.1016/S0014-5793(98)00652-8.

He, Z., Xie, W.J., Liu, Z., Liu, G., Wang, Z., Gao, Y.Q., and Wang, J. (2016). Tuning ice nucleation with counterions on polyelectrolyte brush surfaces. Sci. Adv *2*. https://doi.org/10.1126/sciadv.1600345.

He, Z., Liu, K., and Wang, J. (2018). Bioinspired materials for controlling ice nucleation, growth, and recrystallization. Acc. Chem. Res. *51*, 1082–1091. https://doi.org/10.1021/acs.accounts.7b00528.

Hew, C.L., Slaughter, D., Fletcher, G.L., and Joshi, S.B. (1981). Antifreeze glycoproteins in the plasma of Newfoundland Atlantic cod (Gadus morhua). Can. J. Zool. *59*, 2186–2192. https://doi.org/10.1139/z81-296.

Hill, J.O. (1991). For Better Thermal Analysis and Calorimetry, 3rd ed. (ICTAC).

D.K. Hincha, and E. Zuther, eds. (2014). In Plant Cold Acclimation Methods and Protocols Methods in Molecular Biology, *1166* (Springer Protocols).

Hiranuma, N., Adachi, K., Bell, D.M., Belosi, F., Beydoun, H., Bhaduri, B., Bingemer, H., Budke, C., Clemen, H.C., Conen, F., et al. (2019). A comprehensive characterization of ice nucleation by three different types of cellulose particles immersed in water. Atmos. Chem. Phys. *19*, 4823–4849. https://doi.org/10.5194/acp-19-4823-2019.

Hoshino, T., Kiriaki, M., Ohgiya, S., Fujiwara, M., Kondo, H., Nishimiya, Y., Yumoto, I., and Tsuda, S. (2003). Antifreeze proteins from snow mold fungi. Can. J. Bot. *81*, 1175–1181. https://doi.org/10.1139/b03-116.

Huang, M.L., Ehre, D., Jiang, Q., Hu, C., Kirshenbaum, K., and Ward, M.D. (2012). Biomimetic peptoid oligomers as dual-action antifreeze agents. Proc. Natl. Acad. Sci. U S A *109*, 19922–19927. https://doi.org/10.1073/pnas.1212826109.

Hudait, A., Moberg, D.R., Qiu, Y., Odendahl, N., Paesani, F., and Molinero, V. (2018). Preordering of water is not needed for ice recognition by hyperactive antifreeze proteins. Proc. Natl. Acad. Sci. U S A *115*, 8266–8271. https://doi.org/10.1073/pnas.1806996115.

Inada, T., and Lu, S.S. (2004). Thermal hysteresis caused by non-equilibrium antifreeze activity of poly (vinyl alcohol). Chem. Phys. Lett. *394*, 361–365. https://doi.org/10.1016/j.cplett.2004.07.021.

Ishibe, T., Congdon, T., Stubbs, C., Hasan, M., Sosso, G.C., and Gibson, M.I. (2019). Enhancement of macromolecular ice recrystallization inhibition activity by exploiting depletion forces. ACS Macro Lett. *8*, 1063–1067. https://doi.org/10.1021/acsmacrolett.9b00386.

Jia, Z., DeLuca, C.I., Chao, H., and Davies, P.L. (1996). Structural basis for the binding of a globular antifreeze protein to ice. Chemtracts *384*, 285–288. https://doi.org/10.1038/384285a0.

Jiang, S., and Nail, S.L. (1998). Effect of process conditions on recovery of protein activity after freezing and freeze-drying. Eur. J. Pharm. Biopharm. *45*, 249–257. https://doi.org/10.1016/S0939-6411(98)00007-1.

Kaleda, A., Tsanev, R., Klesment, T., Vilu, R., and Laos, K. (2018). Ice cream structure modification by ice-binding proteins. Food Chem. *246*, 164–171. https://doi.org/10.1016/j.foodchem.2017.10.152.

Kasper, J.C., and Friess, W. (2011). The freezing step in lyophilization: physico-chemical fundamentals, freezing methods and consequences on process performance and quality attributes of biopharmaceuticals. Eur. J. Pharm. Biopharm. *78*, 248–263. https://doi.org/10.1016/j.ejpb.2011.03.010.

Kent, R.A., Andersen, D., Caux, P.Y., and Teed, S. (1999). Canadian water quality guidelines for glycols - an ecotoxicological review of glycols and associated aircraft anti-icing and deicing fluids. Environ. Toxicol. *14*, 481–522. https://doi.org/10.1002/(SICI)1522-7278(199912)14:5<481::AID-TOX5>3.0.CO;2-8.

Kiani, H., and Sun, D.W. (2011). Water crystallization and its importance to freezing of foods: a review. Trends Food Sci. Technol. *22*, 407–426. https://doi.org/10.1016/j.tifs.2011.04.011.

Knight, C.A., and Duman, J.G. (1986). Inhibition of recrystallization of ice by insect thermal hysteresis proteins: a possible cryoprotective role. Cryobiology *23*, 256–262. https://doi.org/10.1016/0011-2240(86)90051-9.

Knight, C.A., Wen, D., and Laursen, R.A. (1995). Nonequilibrium antifreeze peptides and the recrystallization of ice. Cryobiology *32*, 23–34. https://doi.org/10.1006/cryo.1995.1002.

Kristiansen, E., Pedersen, S.A., and Zachariassen, K.E. (2008). Salt-induced enhancement of antifreeze protein activity: a salting-out effect. Cryobiology *57*, 122–129. https://doi.org/10.1016/j.cryobiol.2008.07.001.

Leiter, A., Rau, S., Winger, S., Muhle-Goll, C., Luy, B., and Gaukel, V. (2016). Influence of heating temperature, pressure and pH on recrystallization inhibition activity of antifreeze protein type III. J. Food Eng. *187*, 53–61. https://doi.org/10.1016/j.jfoodeng.2016.04.019.

Leiter, A., Emmer, P., and Gaukel, V. (2018). Influence of gelation on ice recrystallization inhibition activity of kappa-carrageenan in sucrose solution. Food Hydrocolloids *76*, 194–203. https://doi.org/10.1016/j.foodhyd.2016.11.028.

Li, N., Andorfer, C.A., and Duman, J.G. (1998). Enhancement of insect antifreeze protein activity by solutes of low molecular mass. J. Exp. Biol. *201*, 2243–2251. https://doi.org/10.1242/jeb.201.15.2243.

Li, T., Zhao, Y., Zhong, Q., and Wu, T. (2019). Inhibiting ice recrystallization by nanocelluloses. Biomacromolecules *20*, 1667–1674. https://doi.org/10.1021/acs.biomac.9b00027.

Li, T., Li, M., Zhong, Q., and Wu, T. (2020). Effect of fibril length on the ice recrystallization inhibition activity of nanocelluloses. Carbohydr. Polym. *240*, 116275. https://doi.org/10.1016/j.carbpol.2020.116275.

Liou, Y.C., Thibault, P., Walker, V.K., Davies, P.L., and Graham, L.A. (1999). A complex family of highly heterogeneous and internally repetitive hyperactive antifreeze proteins from the beetle Tenebrio molitor. Biochemistry *38*, 11415–11424. https://doi.org/10.1021/bi990613s.

Liu, L., Shen, D., Chen, H., Sun, W., Qian, Z., Zhao, H., and Jiang, J. (2014). Analysis of damage development in cement paste due to ice nucleation at different temperatures. Cem. Concr. Compos. *53*, 1–9. https://doi.org/10.1016/j.cemconcomp.2014.06.007.

Liu, Z., Li, H., Pang, H., Ma, J., and Mao, X. (2015). Enhancement effect of solutes of low molecular mass on the insect antifreeze protein ApAFP752 from Anatolica polita. J. Therm. Anal. Calorim. *120*, 307–315. https://doi.org/10.1007/s10973-014-4171-y.

Lu, M., Wang, B., Li, Z., Fei, Y., Wei, L., and Gao, S. (2002). Differential scanning calorimetric and circular dichroistic studies on plant antifreeze proteins. J. Therm. Anal. Calorim. https://doi.org/10.1023/A:1014369208229.

Mahatabuddin, S., Hanada, Y., Nishimiya, Y., Miura, A., Kondo, H., Davies, P.L., and Tsuda, S. (2017). Concentration-dependent oligomerization of an alpha-helical antifreeze polypeptide makes it hyperactive. Sci. Rep. *7*, 42501–42509. https://doi.org/10.1038/srep42501.

Marshall, C.B., Fletcher, G.L., and Davies, P.L. (2004). Hyperactive antifreeze protein in a fish. Nature *429*, 153. https://doi.org/10.1038/429153a.

Mitchell, D.E., Lilliman, M., Spain, S.G., and Gibson, M.I. (2014). Quantitative study on the antifreeze protein mimetic ice growth inhibition properties of poly(ampholytes) derived from vinyl-based polymers. Biomater. Sci. *2*, 1787–1795. https://doi.org/10.1039/c4bm00153b.

Mitchell, D.E., Cameron, N.R., and Gibson, M.I. (2015). Rational, yet simple, design and synthesis of an antifreeze-protein inspired polymer for cellular cryopreservation. Chem. Commun. *51*, 12977–12980. https://doi.org/10.1039/c5cc04647e.

Mitchell, D.E., Fayter, A.E.R.R., Deller, R.C., Hasan, M., Gutierrez-Marcos, J., and Gibson, M.I. (2019). Ice-recrystallization inhibiting polymers protect proteins against freeze-stress and enable glycerol-free cryostorage. Mater. Horizons *6*, 364–368. https://doi.org/10.1039/C8MH00727F.

Mizrahy, O., Bar-Dolev, M., Guy, S., and Braslavsky, I. (2013). Inhibition of ice growth and recrystallization by zirconium acetate and zirconium acetate hydroxide. PLoS One *8*, e59540. https://doi.org/10.1371/journal.pone.0059540.

Moffatt, B., Ewart, V., and Eastman, A. (2006). Cold comfort: plant antifreeze proteins. Physiol. Plant *126*, 5–16. https://doi.org/10.1111/j.1399-3054.2006.00618.x.

Momma, K., and Izumi, F. (2011). VESTA 3 for three-dimensional visualization of crystal, volumetric and morphology data. J. Appl. Crystallogr. *44*, 1272–1276. https://doi.org/10.1107/S0021889811038970.

John Morris, G., and Acton, E. (2013). Controlled ice nucleation in cryopreservation - a review. Cryobiology *66*, 85–92. https://doi.org/10.1016/j.cryobiol.2012.11.007.

Naullage, P.M., Lupi, L., and Molinero, V. (2017). Molecular recognition of ice by fully flexible molecules. J. Phys. Chem. C *121*, 26949–26957. https://doi.org/10.1021/acs.jpcc.7b10265.

Naullage, P.M., and Molinero, V. (2020). Slow propagation of ice binding limits the ice-recrystallization inhibition efficiency of PVA and other flexible polymers. J. Am. Chem. Soc. *142*, 4356–4366. https://doi.org/10.1021/jacs.9b12943.

O'Sullivan, D., Murray, B.J., Ross, J.F., Whale, T.F., Price, H.C., Atkinson, J.D., Umo, N.S., and Webb, M.E. (2015). The relevance of nanoscale biological fragments for ice nucleation in clouds. Sci. Rep. *5*, 8082–8087. https://doi.org/10.1038/srep08082.

O'Sullivan, D., Murray, B.J., Ross, J.F., and Webb, M.E. (2016). The adsorption of fungal ice-nucleating proteins on mineral dusts: a terrestrial reservoir of atmospheric ice-nucleating particles. Atmos. Chem. Phys. *16*, 7879–7887. https://doi.org/10.5194/acp-16-7879-2016.

Olijve, L.L.C.C., Oude Vrielink, A.S., and Voets, I.K. (2016). A simple and quantitative method to evaluate ice recrystallization kinetics using the circle hough transform algorithm. Cryst. Growth Des. *16*, 4190–4195. https://doi.org/10.1021/acs.cgd.5b01637.

Ptitsyn, O.B. (1987). Protein folding: hypotheses and experiments. J. Protein Chem. *6*, 273–293. https://doi.org/10.1007/BF00248050.

Qu, Z., Qu, Z., Suris-Valls, R., Yu, Q., Voets, I.K., Spronken, C.C.M., and Guo, S. (2020). Enhancing the freeze-thaw durability of concrete through ice recrystallization inhibition by poly(vinyl alcohol). ACS Omega *5*, 12825–12831. https://doi.org/10.1021/acsomega.0c00555.

Rahman, S., and Grasley, Z. (2014). A poromechanical model of freezing concrete to elucidate damage mechanisms associated with substandard aggregates. Cem. Concr. Res. *55*, 88–101. https://doi.org/10.1016/j.cemconres.2013.10.001.

Ren, R., Jiang, X., Di, W., Li, Z., Li, B., Xu, J., and Liu, Y. (2019). HSP70 improves the viability of cryopreserved Paeonia lactiflora pollen by regulating oxidative stress and apoptosis-like programmed cell death events. Plant Cell Tissue Organ Cult. *139*, 53–64. https://doi.org/10.1007/s11240-019-01661-z.

Scherer, G.W., and Valenza, J.J. (2005). Mechanisms of frost damage. Mater. Sci. Concr. *7*, 209–246.

Scherer, G.W. (1999). Crystallization in pores. Cem. Concr. Res. *29*, 1347–1358. https://doi.org/10.1016/S0008-8846(99)00002-2.

Slaughter, D., Fletcher, G.L., Ananthanarayanan, V.S., and Hew, C.L. (1981). Antifreeze proteins from the sea raven, Hemitripterus americanus. Further evidence for diversity among fish polypeptide antifreezes. J. Biol. Chem. *256*, 2022–2026. https://doi.org/10.1016/s0021-9258(19)69910-2.

Soukoulis, C., and Fisk, I. (2016). Innovative ingredients and emerging technologies for controlling ice recrystallization, texture, and structure stability in frozen dairy desserts: a review. Crit. Rev. Food Sci. Nutr. *56*, 2543–2559. https://doi.org/10.1080/10408398.2013.876385.

Stubbs, C., Lipecki, J., and Gibson, M.I. (2017). Regioregular alternating polyampholytes have enhanced biomimetic ice recrystallization activity compared to random copolymers and the role of side chain versus main chain hydrophobicity. Biomacromolecules *18*, 295–302. https://doi.org/10.1021/acs.biomac.6b01691.

Stubbs, C., Wilkins, L.E., Fayter, A.E.R., Walker, M., and Gibson, M.I. (2018). Multivalent presentation of ice recrystallization inhibiting polymers on nanoparticles retains activity. Langmuir *35*, 7347–7353. https://doi.org/10.1021/acs.langmuir.8b01952.

Stubbs, C., Congdon, T.R., and Gibson, M.I. (2019). Photo-polymerisation and study of the ice recrystallisation inhibition of hydrophobically modified poly(vinyl pyrrolidone) co-polymers. Eur. Polym. J. *110*, 330–336. https://doi.org/10.1016/j.eurpolymj.2018.11.047.

Suris-Valls, R., and Voets, I.K. (2019). The impact of salts on the ice recrystallization inhibition activity of antifreeze (glyco) proteins. Biomolecules *9*, 347. https://doi.org/10.3390/biom9080347.

Tab, M.M., Hashim, N.H.F., Najimudin, N., Mahadi, N.M., Bakar, F.D.A., and Murad, A.M.A. (2018). Large-scale production of glaciozyma Antarctica antifreeze protein 1 (Afp1) by fed-batch fermentation of Pichia pastoris. Arab J. Sci. Eng. *43*, 133–141. https://doi.org/10.1007/s13369-017-2738-1.

Tomalty, H.E., Graham, L.A., Eves, R., Gruneberg, A.K., and Davies, P.L. (2019). Laboratory-scale isolation of insect antifreeze protein for cryobiology. Biomolecules *9*, 180. https://doi.org/10.3390/biom9050180.

Tomczak, M.M., Marshall, C.B., Gilbert, J.A., and Davies, P.L. (2003). A facile method for determining ice recrystallization inhibition by antifreeze proteins. Biochem. Biophys. Res. Commun. *311*, 1041–1046. https://doi.org/10.1016/j.bbrc.2003.10.106.

United States Geological Survey (USGS) (2022). Industrial water use. https://www.usgs.gov/mission-areas/water-resources/science/industrial-water-use?qt-science_center_objects=0#qt-science_center_objects.

Vance, T.D.R.R., Graham, L.A., and Davies, P.L. (2018). An ice binding and tandem beta sandwich domain containing protein in *Shewanella frigidimarina* is a potential new type of ice adhesin. FEBS J. *285*, 1511–1527. https://doi.org/10.1111/febs.14424.

Voets, I.K. (2017). From ice-binding proteins to bio-inspired antifreeze materials. Soft Matter *13*, 4808–4823. https://doi.org/10.1039/c6sm02867e.

Voitkovskii, K.F. (1960). Translation of the mechanical properties of ice. https://apps.dtic.mil/dtic/tr/fulltext/u2/284777.pdf.

Wang, L., and Duman, J.G. (2006). A thaumatin-like protein from larvae of the beetle Dendroides canadensis enhances the activity of antifreeze proteins. Biochemistry *45*, 1278–1284. https://doi.org/10.1021/bi051680r.

Wang, Z., Wang, Z., Liu, D., Jing, L., Gao, C., Li, J., He, Z., Wang, J., Chen, Z., and Yang, B. (2020). Bioinspired cryoprotectants of glucose-based carbon dots. ACS Appl. Bio Mater. *3*, 3785–3791. https://doi.org/10.1021/acsabm.0c00376.

Whale, T.F., Murray, B.J., O'Sullivan, D., Wilson, T.W., Umo, N.S., Baustian, K.J., Atkinson, J.D., Workneh, D.A., and Morris, G.J. (2015). A technique for quantifying heterogeneous ice nucleation in microlitre supercooled water droplets. Atmos. Meas. Tech. *8*, 2437–2447. https://doi.org/10.5194/amt-8-2437-2015.

Worrall, D., Elias, L., Ashford, D., Smallwood, M., Sidebottom, C., Lillford, P., Telford, J., Holt, C., and Bowles, D. (1998). A carrot leucine-rich-repeat protein that inhibits ice recrystallization. Science *282*, 115–117. https://doi.org/10.1126/science.282.5386.115.

Wu, D.W., and Duman, J.G. (1991). Activation of antifreeze proteins from larvae of the beetle Dendroides canadensis. J. Comp. Physiol. B *161*, 279–283. https://doi.org/10.1007/BF00262309.

Wu, S., Zhu, C., He, Z., Xue, H., Fan, Q., Song, Y., Francisco, J.S., Zeng, X.C., and Wang, J. (2017). Ion-specific ice recrystallization provides a facile approach for the fabrication of porous materials. Nat. Commun. *8*, 15154–15158. https://doi.org/10.1038/ncomms15154.

Xiao, N., Suzuki, K., Nishimiya, Y., Kondo, H., Miura, A., Tsuda, S., and Hoshino, T. (2010). Comparison of functional properties of two fungal antifreeze proteins from Antarctomyces psychrotrophicus and Typhula ishikariensis. FEBS J. *277*, 394–403. https://doi.org/10.1111/j.1742-4658.2009.07490.x.

Xue, B., Zhao, L., Qin, X., Qin, M., Lai, J., Huang, W., Lei, H., Wang, J., Wang, W., Li, Y., and Cao, Y. (2019). Bioinspired ice growth inhibitors based on self-assembling peptides. ACS Macro Lett. *8*, 1383–1390. https://doi.org/10.1021/acsmacrolett.9b00610.

Yang, R., Lemarchand, E., Fen-Chong, T., and Azouni, A. (2015). A micromechanics model for partial freezing in porous media. Int. J. Solids. Struct. *75–76*, 109–121. https://doi.org/10.1016/j.ijsolstr.2015.08.005.

Yang, H.G., Ma, C., Li, K.Y., Liu, K., Loznik, M., Teeuwen, R., van Hest, J.C.M., Zhou, X., Herrmann, A., and Wang, J. (2016). Tuning ice nucleation with supercharged polypeptides. Adv. Mater. *28*, 5008–5012. https://doi.org/10.1002/adma.201600496.

Zanetti-Polzi, L., Biswas, A.D., Del Galdo, S., Barone, V., and Daidone, I. (2019). Hydration shell of antifreeze proteins: unveiling the role of non-ice-binding surfaces. J. Phys. Chem. B *123*, 6474–6480. https://doi.org/10.1021/acs.jpcb.9b06375.

Zhang, D.Q., Liu, B., Feng, D.R., He, Y.M., and Wang, J.F. (2004). Expression, purification, and antifreeze activity of carrot antifreeze protein and its mutants. Protein Expr. Purif. *35*, 257–263. https://doi.org/10.1016/j.pep.2004.01.019.

Zhang, W., and Laursen, R.A. (1999). Artificial antifreeze polypeptides: α-Helical peptides with KAAK motifs have antifreeze and ice crystal morphology modifying properties. FEBS Lett. *455*, 372–376. https://doi.org/10.1016/S0014-5793(99)00906-0.